Polymer Chemistry

Accepted Manuscript

This is an *Accepted Manuscript*, which has been through the Royal Society of Chemistry peer review process and has been accepted for publication.

Accepted Manuscripts are published online shortly after acceptance, before technical editing, formatting and proof reading. Using this free service, authors can make their results available to the community, in citable form, before we publish the edited article. We will replace this *Accepted Manuscript* with the edited and formatted *Advance Article* as soon as it is available.

You can find more information about *Accepted Manuscripts* in the Information for Authors.

Please note that technical editing may introduce minor changes to the text and/or graphics, which may alter content. The journal's standard Terms & Conditions and the Ethical guidelines still apply. In no event shall the Royal Society of Chemistry be held responsible for any errors or omissions in this *Accepted Manuscript* or any consequences arising from the use of any information it contains.

ROYAL SOCIETY OF CHEMISTRY

www.rsc.org/polymers

Journal Name

COMMUNICATION

Supramolecular polymerization induced self-assembly into micelle and vesicle *via* acid-base controlled formation of fluorescence responsive supramolecular hyperbranched polymers

Received 00th January 20xx,
Accepted 00th January 20xx

DOI: 10.1039/x0xx00000x

www.rsc.org/

Lijie Li, Xiaorui Zheng, Bingran Yu, Lipeng He, Jing Zhang, Haomin Liu, Yong Cong and Weifeng Bu*

Two asymmetric conjugated monomers of AB_2-1 and AB_2-2 with both dibenzo-24-crown-8 and dibenzylamine groups can self-assemble to form micellar and vesicular aggregates under an acid condition, during which supramolecular hyperbranched polymers form controllably *via* host–guest recognition between dibenzo-24-crown-8 and dibenzylammonium groups.

By associating monomeric units through noncovalent interactions, supramolecular polymers can be achieved with typical features of conventional polymers in both solution and bulk.[1] The dynamic nature of noncovalent interactions affords them really reversible and responsive upon triggering by external stimuli. The molecular weight increases with the increase in the monomer concentration. On the other hand, with a soluble macromolecular initiator, amphiphilic block copolymers result by polymerizing immiscible or miscible monomers to obtain an insoluble block in situ, leading to polymerization-induced self-assembly (PISA) of the diblock copolymers into micellelike nanoobjects with controllable morphologies and desired functions.[2] Similarly, by noncovalently initiating a monomer bearing both an anionic host and a cationic guest by a polymeric initiator of anionic host terminated poly(ethylene glycol), supramolecular block copolymers are generated in situ with controllable block ratios and further self-assemble sequentially to form spheres, discs and vesicles in water.[3] Here, for the first time, we report the total supramolecular PISA of supramolecular hyperbranched polymers (SHPs) produced in situ by π-conjugated AB_2 monomers with both dibenzo-24-crown-8 (DB24C8) and dibenzylamine groups into micellar and vesicular aggregates under an acid condition.

The synthetic routes toward asymmetric conjugated monomers of **AB_2-1** and **AB_2-2** were described in Scheme 1. The rigid triangular structure of **5** with six alkyl chains was synthesized by Sonogashira cross-coupling reaction of **3**[4a] with 1,3,5-triethynylbenzene[4b] and sequential TMS desilylation. Sonogashira coupling of **5** with 4-iodobenzaldehyde afforded **6a** and **6b**, which were converted successively to **8a** and **8b**, respectively, by Sonogashira coupling with **6**.[4c] The treatments of **8a** and **8b** with benzylamine produced the imine compounds of **9a** and **9b**, which were reduced with sodium borohydride to afford the target monomers of **AB_2-1** and **AB_2-2**, respectively. They were fully characterized by ^{1}H and ^{13}C NMR spectra together with high-resolution electrospray ionization mass spectra (Fig. S13-S18 and Fig. 1a).

The supramolecular polymerization of **AB_2-2** to **PAB_2-2** was first analyzed by ^{1}H NMR spectra. Upon adding slightly excessive hexafluorophosphoric acid (HFA, 2.4 equiv.) into the CD_2Cl_2 solution of **AB_2-2** with a concentration of 2.14×10^{-3} mol L^{-1}, three new broad bands appeared at δ = 4.5, 4.7, and 4.9 ppm (Fig. 1a and b). According to previously reported ^{1}H NMR results on host–guest recognition between DB24C8 and dibenzylammonium,[5] they were assigned clearly to the benzylic methylene protons ($H_{\theta c}$+H_{vc}) adjacent to the NH_2^+ centres hosted by the DB24C8 moieties at linear units, terminal units, and dendritic units, respectively. Their respective integrals allowed us to approximately calculate the degrees of branching (DB) of 80±8% and 70±7% at concentrations of 2.14×10^{-3} and 2.14×10^{-4} molL^{-1} (Fig. S19), respectively, according to the following equation: DB = [(no. of dendritic units) + (no. of terminal units)]/(total no. of units).[6] The proton signals of the crown ether became much more complicated and broader and ranged from δ = 3.2 to 4.3 ppm, and were overlapped with those resonances of the methylene protons (δ = 3.8–3.9 ppm) adjacent to the uncomplexed dibenzylammonium groups and the conjugated core. Furthermore, the proton resonances in the conjugated core were similarly broadened, complicated, and upfield shifted significantly. These ^{1}H NMR spectral features revealed that

Key Laboratory of Nonferrous Metals Chemistry and Resources Utilization of Gansu Province, State Key Laboratory of Applied Organic Chemistry and College of Chemistry and Chemical Engineering, Lanzhou University, Lanzhou, Gansu, China, E-mail: buwf@lzu.edu.cn

Electronic Supplementary Information (ESI) available: Synthesis and characterization details of all compounds, additional DLS data and TEM images. See DOI: 10.1039/x0xx00000x

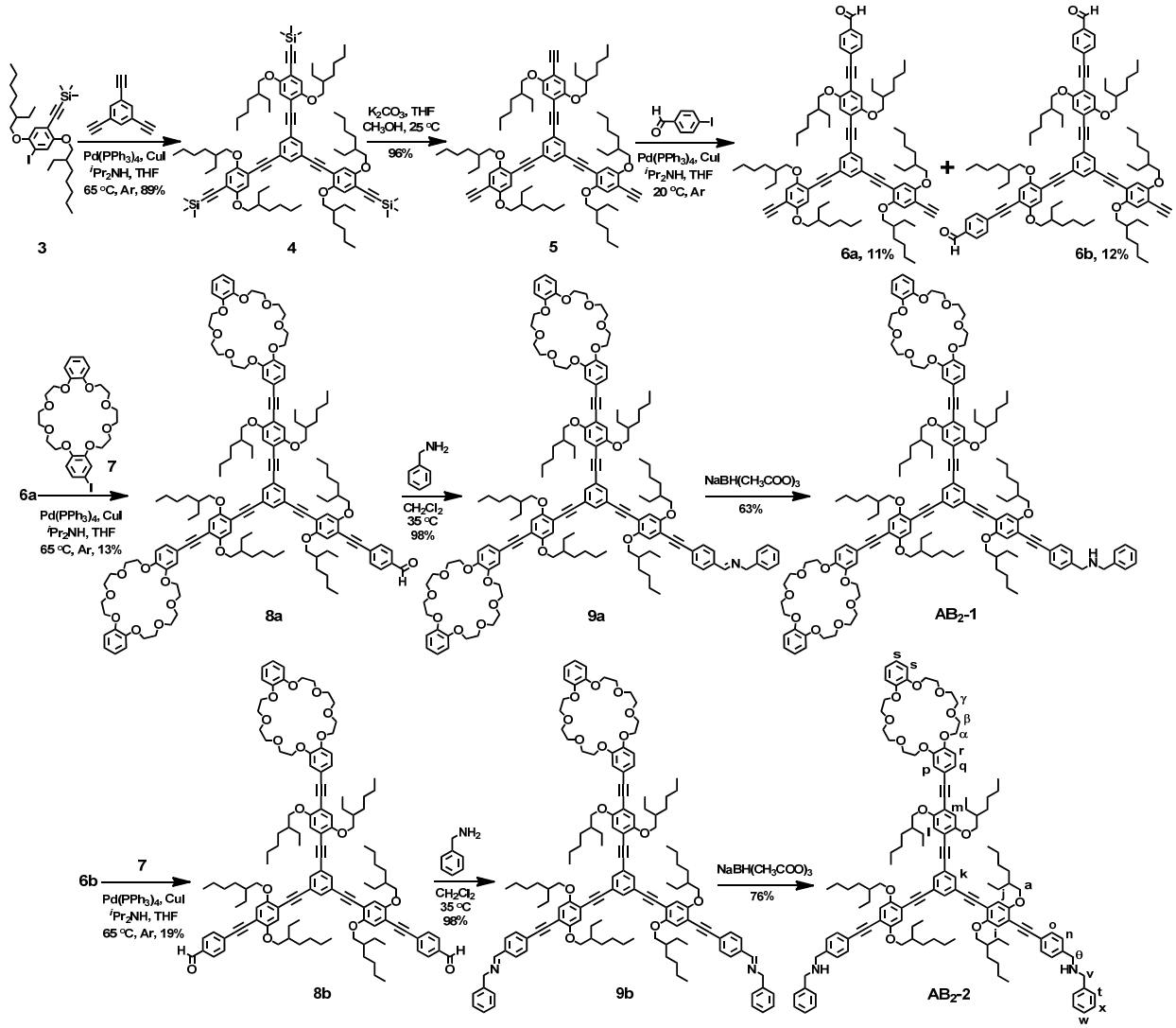

Scheme 1. The synthetic routes of **AB_2-1** and **AB_2-2**. The synthesis and characterization was detailed in the ESI part.

almost all of the DB24C8 moieties were threaded by the dibenzylammonium ions and thus the SHP of **PAB_2-2** formed under this acid condition. The significant upfield shift of the proton signals in the conjugated core was accordingly attributed to the presence of rather strong π-π stacking interactions in **PAB_2-2**,[5h,7] which was further supported by the fluorescence spectral studies as addressed below.

The independent signal at 7.09 ppm was due to the complexed H_{wc} and the uncomplexed H_{wu} cannot be clearly assigned because of the highly overlapping resonances. The former together with the total H_w (H_{wc} + H_{wu}) could be used as a standard to calculate the percentage recognition (*p*) and polymerization degree (*n*): $p = A(H_{\theta c}+H_{vc})/2A(H_{wc}+H_{wu}) = n/(n+1)$, in which $A(H_{\theta c}+H_{vc})$ and $A(H_{wc}+H_{wu})$ are the average intergrals of ($H_{\theta c}+H_{vc}$) and ($H_{wc}+H_{wu}$), respectively.[5c,h,i,8] Accordingly, the values of *p* and *n* were estimated to be 98.8 ± 0.2% and 83 ± 13 at a concentration of 2.14×10^{-3} mol L^{-1} and be 96.3 ± 0.2% and 27 ± 1 at a concentration of 2.14×10^{-4} mol L^{-1} (Fig. S19), which corresponded respectively to the molecular weights of $(1.95\pm0.31)\times10^5$ and $(6.34\pm0.24)\times10^4$ g mol^{-1}. When the concentration further decreased, the calculated values of *p* and *n* occupied large errors certainly because of the much weaker ^{1}H NMR signals. To validate the supramolecular polymerization, diffusion-ordered ^{1}H NMR spectroscopy (DOSY) was performed to measure the size evolution. At a concentration of 2.14×10^{-3} mol L^{-1}, single bands occurred respectively at log*D* = -8.14 and -8.83 for **AB_2-2** and **PAB_2-2**, demonstrating an appreciable size increase from **AB_2-2** to **PAB_2-2** as a result of the successful supramolecular polymerization (Fig. S20a and b). When slightly excessive *N*-tert-butyl-*N',N',N'',N'',N''',N'''*-hexamethylphosphorimidic triamide (P_1-*t*Bu, 2.8 equiv.) was added to the same solution, both the ^{1}H NMR signals and log*D* were completely regenerated (Fig. 2c and Fig. S20c), indicative of the highly reversible formation of **PAB_2-2**.

To support the aforementioned π-π stacking interaction, fluorescence behaviours were further investigated. Upon excitation at 370 nm, the solution of **AB_2-2** in CH_2Cl_2 (1.57×10^{-5} mol L^{-1}) exhibited two strong fluorescence bands at λ = 416 and 436 nm typically due to a monomeric excited state of the

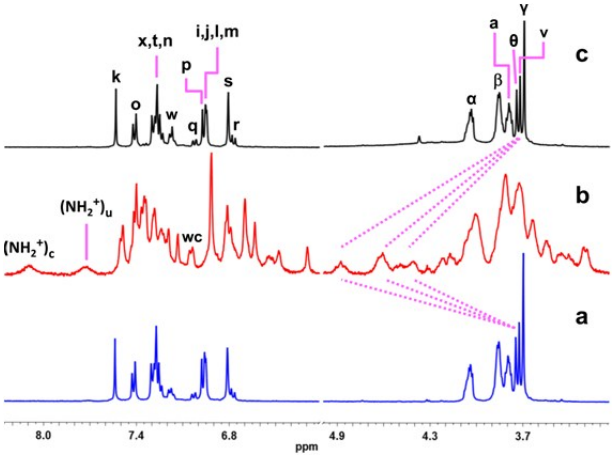

Fig. 1 Partial ^{1}H NMR spectra (400 MHz, CD_2Cl_2, 2.14×10^{-3} mol L^{-1}) of **AB_2-2** (a), **PAB_2-2** (b) obtained by adding 2.4 equivalents of HFA to the solution of **AB_2-2**, and **AB_2-2** (c) obtained by adding 2.8 equivalents of P_1-*t*Bu to the solution of **PAB_2-2**.

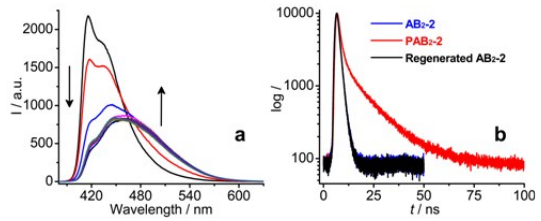

Fig. 2 (a) Fluorescence spectral changes of **AB_2-2** (CH_2Cl_2, 1.57×10^{-5} mol L^{-1}) upon titration with HFA. (b) Fluorescence decay profiles of **AB_2-2**, **PAB_2-2**, and regenerated **AB_2-2** excited at 370 nm at room temperature.

conjugated core (Fig. 2a). Upon dropwise adding HFA to this solution, the fluorescence intensities decreased significantly and red shift to 422 and 446 nm together with a significant increase in fluorescence intensity of a lower-energy shoulder ranging from 470 to 580 nm. These changes reached their maximum extents at a molar ratio of 2/1 between HFA and **AB_2-2** (Fig. S21). The former bathochromic shift was due to the tunable electronic conformation of the conjugated core by the [N^+–H···O] and [C–H···O] hydrogen bonds of the host–guest recognition between DB24C8 and dibenzylammonium, while the latter low-energy shoulder was characteristic of an excimeric emission originating from the π-π stacking interactions among the conjugated cores. Upon excitation again at 370 nm, the fluorescence decay of **AB_2-2** was single exponential with a lifetime of 1.30 ns (Fig. 2b and Table S1). Of difference was that **PAB_2-2** occupied a double exponential decay with lifetimes of 1.47 and 12.46 ns and their relative weighting ratios were 44.92% and 55.08%, respectively (Fig. 2b and Table S1). They stemmed from the excited states of monomer and excimers, respectively. The latter was a typical result of the formation of **PAB_2-2** and thus the rather strong π-π stacking interaction between the conjugated cores there. After adding 2.8 equivalents of P_1-*t*Bu to the solution of **PAB_2-2**, the fluorescence spectrum (Fig. S22) and decay curve (Fig. 2b and Table S1) reverted completely to the original state of **AB_2-2**, again revealed the reversible fabrication of the SHP.

The SHP of **PAB_2-2** was further examined by concentration dependent dynamic light scattering (DLS) measurements. The hydrodynamic diameter (D_h) of **AB_2-2** was 4 nm, consistent with its molecular size. With concentrations increased from 2.14×10^{-5} to 2.14×10^{-4} to 2.14×10^{-3} mol L^{-1}, D_h of **PAB_2-2** increased from 18 and 75 to 42 and 173 to 382 nm, respectively (Fig. 3a), much larger than D_h of **AB_2-2** (4 nm). This together with the above concentration dependent ^{1}H NMR data displayed a typical supramolecular polymerization process. After adding a slightly excessive of P_1-*t*Bu, D_h returned back to 3.5 nm, agreeing well with the reversible formation of **PAB_2-2** (Fig. 3a).

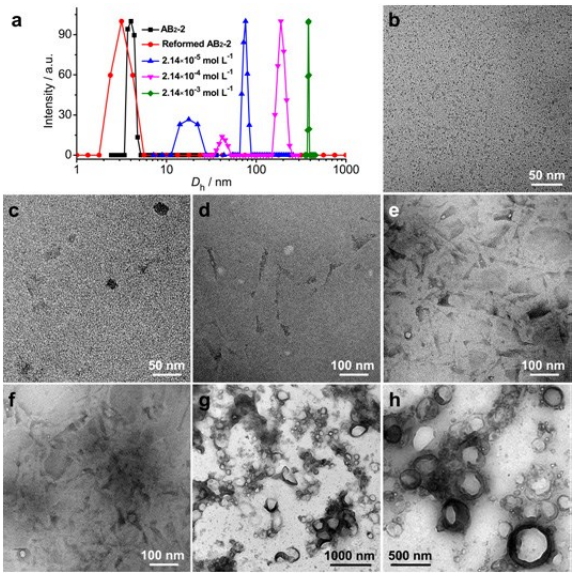

Fig. 3 (a) DLS curves of **AB_2-2**, reformed **AB_2-2**, and **PAB_2-2** obtained at different concentrations. TEM images of **AB_2-2** (b) and **PAB_2-2** at concentrations of 2.14×10^{-5} mol L^{-1} (c and d), 2.14×10^{-4} mol L^{-1} (e and f) and 2.14×10^{-3} mol L^{-1} (g and h).

The CH_2Cl_2 solution of **AB_2-2** and **PAB_2-2** were cast onto carton-coated copper grids for transmission electron microscopy (TEM) observations. In a typical TEM image of **AB_2-2**, nanoparticles with a diameter of ca. 4 nm was clearly observed (Fig. 3b), conforming to its molecular size and D_h. At a concentration of 2.14×10^{-5} mol L^{-1}, the TEM images revealed that rodlike aggregates formed with a length of ca. 100 nm and a width of ca. 20 nm and coexisted with nanoparticles with a diameter of ca. 15 nm (Fig. 3c and d). When the concentration increased to 2.14×10^{-4} mol L^{-1}, **PAB_2-2** formed sheetlike aggregates with a broad size distribution from 30 to 150 nm (Fig. 3e and f). The smaller sizes of the nanoparticles in the TEM images of Fig. 3c-f were lined closely up with the fast modes at 18 and 42 nm in the DLS patterns obtained from the solutions of **PAB_2-2** with concentrations of 2.14×10^{-5} mol L^{-1} and 2.14×10^{-4} mol L^{-1}, respectively (Fig. 3a). In the latter case, the polymerization degree *n* of 27 calculated from the ^{1}H NMR spectrum was highly consistent with the smaller sized nanoparticles obtained from both DLS and TEM measurements. Therefore, all of these smaller sized nanoparticles were assigned to single supramolecular polymers of **PAB_2-2** at their corresponding concentrations. The aggregates with larger sizes were due to the supramolecular PISA even under these dilute conditions. Occasionally, small

sized vesicles were captured at 2.14×10^{-4} mol L^{-1} (Fig. 3e and f). Additional increase in the concentration to 2.14×10^{-3} mol L^{-1} resulted in the formation of vesicles (Fig. 3g and h). The diameter and thickness ranged respectively from 150 to 650 nm and from 12 to 55 nm. The concentration dependent size evolution from TEM images was consistent with the DLS results mentioned above. However, for the first time, supramolecular PISA occurred to form vesiclelike aggregates by complete noncovalent interactions (Fig. 4).

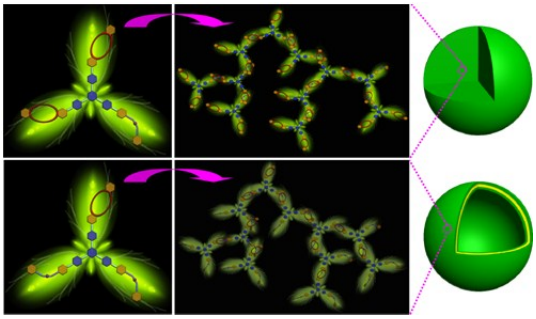

Fig. 4 Supramolecular polymerization of **AB_2-1** and **AB_2-2** into **PAB_2-1** and **PAB_2-2** resulted in the self-assembly to form micellar (top) and vesicular aggregates (bottom), respectively.

Similarly, **PAB_2-1** could be obtained reversibly by the supramolecular polymerization of **AB_2-1** through the acid-base controllable host–guest recognition between DB24C8 and dibenzylammonium groups. Of difference was that **PAB_2-1** occupied the *P* and *n* values of only 91% and 10, respectively, at a concentration of 2.14×10^{-3} mol L^{-1} as suggested by the ^{1}H NMR spectral studies (Fig. S23 and S24). And the proton resonances of the conjugated core were also upshifted, but only slightly in comparison with the cases of **AB_2-2** and **PAB_2-2**. In terms of fluorescence spectra and decays, only slight changes were observed between **AB_2-1** and **PAB_2-1** (Fig. S25, S26 and Table S2). This together with the ^{1}H NMR results indicated that much weaker π-π stacking interaction occurred in **PAB_2-1** than **PAB_2-2**. However, D_h of **PAB_2-1** was 128 nm at a concentration of 2.14×10^{-3} mol L^{-1} (Fig. S27), much larger than those of **AB_2-1** (4 nm) and **PAB_2-1** (12 nm, calculated from n = 10). In a typical TEM image (Fig. S28), micellelike aggregates were clearly observed with an average diameter of 100 nm, which was again due to the supramolecular PISA (Fig. 4). The difference of the aggregate morphologies between **PAB_2-1** and **PAB_2-2** was due to the different hydrophobic/hydrophilic balance in CH_2Cl_2 originating from their different molecular structures: The former possessed a periphery of DB24C8 moieties, while in the latter case, the peripheral area was occupied by dibenzylammonium groups (Fig. 4). This might be why much stronger π-π stacking interaction appeared in **PAB_2-2** than **PAB_2-1**.

In summary, we have synthesized and characterized two asymmetric conjugated monomers of **AB_2-1** and **AB_2-2** containing both DB24C8 and dibenzylamine groups. They can reversibly form the SHPs of **PAB_2-1** and **PAB_2-2** in situ under acid-base controlled reactions *via* host–guest recognition between DB24C8 and dibenzylammonium groups. During the supramolecular polymerization processes, **PAB_2-2** is induced to self-assemble into vesiclelike aggregates, while only micelles form for **PAB_2-1**. This supramolecular PISA together with conjugated monomers will provide an efficient approach to fabricate fluorescence responsive SHPs with controllable aggregate morphologies and thus potential applications in intelligent materials and optical information storage.

This work is supported by the NSFC (51173073), the Fundamental Research Funds for the Central Universities (lzujbky-2014-74 and lzujbky-2015-k04) and the Open Project of State Key Laboratory of Supramolecular Structure and Materials of Jilin University (sklssm201502).

Notes and references

1 (*a*) T. F. A. De Greef, M. M. J. Smulders, M. Wolffs, A. P. H. J. Schenning, R. P. Sijbesma and E. W. Meijer, *Chem. Rev.*, 2009, **109**, 5687; (*b*) L. Yang, X. Tan, Z. Wang and X. Zhang, *Chem. Rev.*, 2015, **115**, 7196; (*c*) M. Xue, Y. Yang, X. Chi, X. Yan and F. Huang, *Chem. Rev.*, 2015, **115**, 7398; (*d*) Z. Zhang, Y. Luo, J. Chen, S. Dong, Y. Yu, Z. Ma and F. Huang, *Angew. Chem., Int. Ed.*, 2011, **50**, 1397; (*e*) S. Dong, Y. Luo, X. Yan, B. Zheng, X. Ding, Y. Yu, Z. Ma, Q. Zhao and F. Huang, *Angew. Chem., Int. Ed.*, 2011, **50**, 1905; (*f*) X. Yan, D. Xu, X. Chi, J. Chen, S. Dong, X. Ding, Y. Yu and F. Huang, Adv. Mater., 2012, 24, 362.

2 (*a*) J.-T. Sun, C.-Y. Hong and C.-Y. Pan, *Polym. Chem.*, 2013, **4**, 873; (*b*) B. Charleux, G. Delaittre, J. Rieger and F. D'Agosto, *Macromolecules*, 2012, **45**, 6753; (*c*) N. J. Warren and S. P. Armes, *J. Am. Chem. Soc.*, 2014, **136**, 10174.

3 X. Ji, S. Dong, P. Wei, D. Xia and F. Huang, *Adv. Mater.*, 2013, **25**, 5725.

4 (*a*) S. Kang, R. J. Ono and C. W. Bielawski, *J. Am. Chem. Soc.*, 2013, **135**, 4984; (*b*) S. Leininger, P. J. Stang and S. Huang, *Organometallics*, 1998, **17**, 3981; (*c*) S. Dixon, R. C. D. Brown and P. A. Gale, *Chem. Commun*., 2007, 3565.

5 (*a*) P. R. Ashton, P. J. Campbell, E. J. T. Chrystal, P. T. Glink, S. Menzer, D. Philp, N. Spencer, J. F. Stoddart, P. A. Tasker and D. J. Williams, *Angew. Chem., Int. Ed. Engl*., 1995, **34**, 1865; (*b*) S. J. Cantrill, G. J. Youn and J. F. Stoddart,. *J. Org. Chem*., 2001, **66**, 6857; (*c*) H. W. Gibson, N. Yamaguchi and J. W. Jones, *J. Am. Chem. Soc.*, 2003, **125**, 3522; (*d*) T. Oku, Y. Furusho and T. Takata, *Angew. Chem. Int. Ed.*, 2004, **43**, 96; (*e*) Z. Ge, J. Hu, F. Huang and S. Liu, *Angew. Chem. Int. Ed.*, 2009, **48**, 1798; (*f*) F. Wang, C. Han, C. He, Q. Zhou, J. Zhang, C. Wang, N. Li and F. Huang, *J. Am. Chem. Soc.*, 2008, **130**, 11254; (*g*) Y.-S. Su, J.-W. Liu, Y. Jiang and C.-F. Chen, *Chem. Eur. J.*, 2011, **17**, 2435; (*h*) B. Yu, B. Wang, S. Guo, Q. Zhang, X. Zheng, H. Lei, W. Liu, W. Bu, Y. Zhang and X. Chen, *Chem. - Eur. J.*, 2013, **19**, 4922; (*i*) B. Yu, S. Guo, L. He and W. Bu, *Chem. Commun.*, 2013, **49**, 3333; (*j*) H. Li, X. Fan, W. Tian, H. Zhang, W. Zhang and Z. Yang, *Chem. Commun.*, 2014, **50**, 14666; (*k*) S. Guo, J. Zhang, B. Wang, Y. Cong, X. Chen and W. Bu, *RSC. Adv.*, 2014, **4**, 51754; (*l*) L. He, J. Liang, Y. Cong, X. Chen and W. Bu, *Chem. Commun.*, 2014, **50**, 10841; (*m*) L. He, X. Liu, J. Liang, Y. Cong, Z. Weng and W. Bu, *Chem. Commun.*, 2015, *51*, 7148; (*n*) X. Ji, Y. Yao, J. Li, X. Yan and F. Huang, *J. Am. Chem. Soc.*, 2013, **135**, 74; (*o*) S. Dong, B. Zheng, D. Xu, X. Yan, M. Zhang and F. Huang, *Adv. Mater*., 2012, **24**, 3191.

6 C. J. Hawker, R. Lee and J. M. J. Fréchet, *J. Am. Chem. Soc.*, 1991, **113**, 4583.

7 J. D. Badjic, C. M. Ronconi, J. F. Stoddart, V. Balzani, S. Silvi and A. Credi, *J. Am. Chem. Soc.*, 2006, **128**, 1489.

8. (*a*) Y. Liu, Z. Wang and X. Zhang, *Chem. Soc. Rev.*, 2012, **41**, 5922; (*b*) C. Li, K. Han, J. Li, Y. Zhang, W. Chen, Y. Yu and X. Jia, *Chem. Eur. J.*, 2013, **19**, 11892; (*c*) C. Li, *Chem. Commun*., 2014, **50**, 12420; (*d*) Y. Bai, X. D. Fan, W. Tian, T. T. Liu, H. Yao, Z. Yang, H. T. Zhang and W. B Zhang, *Polym. Chem.*, 2015, **6**, 732.

Graphical Abstract

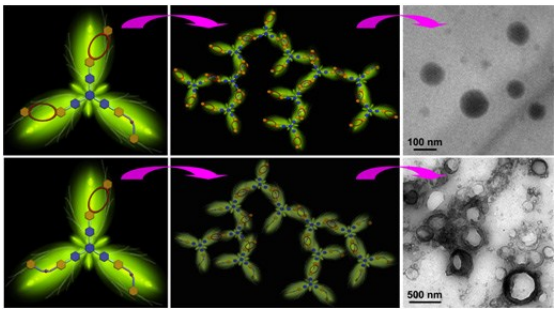

Supramolecular polymerization induced self-assembly into micelle and vesicle *via* acid-base controlled formation of fluorescence responsive supramolecular hyperbranched polymers

Lijie Li, Xiaorui Zheng, Bingran Yu, Lipeng He, Jing Zhang, Haomin Liu, Yong Cong and Weifeng Bu*

Micellar and vesicular aggregates were achieved in situ by supramolecular polymerization of π-conjugated AB_2 monomers with dibenzo-24-crown-8 and dibenzylammonium groups.